Structural, electrical and optical properties of samarium fluoride doped SnO_2 transparent conducting oxide thin films for optoelectronic device applications

Dao Van Da[1], Tran Quang Phu[1*] , Pham Van Hoi[2]

[1]Department of Electrical and Electronic Engineering, Hung Yen University of Technology and Education;
[2]Institute of Materials Science, Vietnam Academy of Science and Technology.
[*]Corresponding author: tranquangphu@utehy.edu.vn

Received 1 Apr. 2023; Revised 18 May 2023; Accepted 10 Jun. 2023 ; Published 25 Jun. 2023.

DOI: https://doi.org/10.54939/1859-1043.j.mst.88.2023.123-130

ABSTRACT

In this study, p-type transparent tin oxide (SnO_2) based semiconductor thin films were deposited onto glass substrates by sol-gel dip-coating method using samarium-trifluoride (SmF_3) as acceptor dopant. The films were prepared by co-doping 2 mol.% of SmF_3 into SnO_2 (SFTO), followed by annealing temperature at 475 $^{\circ}C$. XRD analysis results showed that the films exhibited the tetragonal rutile SnO_2 phase. The p-type conductance of the SFTO films were confimed by Hall effect and Seebeck coefficient measurements. Resistivity and mobility of the SmF_3 doped SnO_2 film is 7.83 × 10^{-3} Ωcm and 7.57 cm^2 V^{-1} s^{-1}, respectively, which reduce in comparing with those of un-doped SnO_2 film. Carrier concentration is large increase from –9.34 × 10^{18} cm^{-3} for un-doped- to +1.05 × 10^{20} cm^{-3} for SmF_3 doped-SnO_2 film. The p-type SFTO film showed a high transmittance of 74.3% at 550 nm, with band gap energy of 3.63 eV. Furthermore, a transparent p-SnO_2:SmF_3/n-ZnO:Al (Al doping level of 2 mol.%) heterojunction was fabricated on alkali-free glass substrates. The I-V curve measurement for the p-n heterojunction diode showed a typical rectifying characteristic with a forward turn-on voltage of 1.55 V. With obtained properties, the p-type SFTO film holds great promise for optoelectronic devices applications.

Keywords: Samarium fluoride co-doped tin oxide films; Transparent conducting oxide (TCO); Sol–gel dip-coating; Electrical resistivity; p-type TCO.

1. INTRODUCTION

The discovery of transparent oxide semiconductors (TOSs) has attracted considerable interest because of their potential applications, is the mile stone in transparent electronics and has paved way for new frontier in the area of optoelectronics. Therefore, transparent conducting oxides (TCO) have been used as key components in many optoelectronic devices such as solar cells, flat panel displays, thin-film transistors, light emitting diodes, energy efficient smart windows, and smart sensors [1, 2]. Most of the highly effective TCOs are n-type in nature, e.g, In-doped SnO_2, F-doped SnO_2, and Al-doped ZnO [3]. Therefore, it is extremely important to develop high-performance p-type TCO for the development of optoelectronic devices. In addition, integration of p-type and n-type oxide semiconductors could lead thin-film transistors (TFT) for Large-Area electronics [4]. To fabricate TCO films suitable for each specific application, multicomponent TCO materials have recently been actively investigated. The advantage of multi-component oxide materials is that alteration of the chemical compositions will alter their electrical, optical, chemical and physical properties. Hui et al. reported p-type AZO:Cu_2O prepared by the sol-gel spin coating method with resistivity (ρ) of 6.94 × 10^{-3} Ω cm and optical transmitance (T_{op}) > 90% [5]. Chien et al. successfully fabricated a Ga-doped SnO_2 p-type semiconductor thin film by sol-gel spin coating method with the highest average hole concentration of 1.70 × 10^{18} cm^{-3} and T_{op} > 87% with optical band gap energy of 3.83 eV. Moreover, the p-type conductivity of the 15% Ga-doped SnO_2 thin film was also confirmed by the non-linear I-V characteristics. Ravichandran

et al. reported a zinc-doped tin oxide film with p-type conductivity prepared by a simplified spray pyrolysis technique. Electrical studies show that the transition from n-type to p-type conductivity occurs when the level of Zn doping changes from 20 to 25 at.% [6]. Recently, Sakthivel et al. reported CdO thin films doped with different rare earth metal ions such as Samarium (Sm), Lanthanum (La) and Neodymium (Nd) deposited on glass substrates by RF sputtering technique, optical and electrical properties of the deposited CdO thin films are elaborately studied [7]. Additionally, thin films of SnO_2 are attracting by its simplicity and the comfort by which it can be produced by number of methods including pulsed laser deposition, chemical vapour deposition, spray pyrolysis, sol-gel process and the DC sputtering [8, 9]. Among the above methods, sol-gel technique followed by considered one of the best technique due to low cost and simplicity of the process for deposition process that offers cost effectiveness, ease of compositional modification, and large-area coating for fabricating functional oxide thin films [10]. Therefore, the first purpose of this work is to study on electrical and optical properties, in particular the conductivity conversion of samarium-trifluoride (SmF_3) compounds doped in SnO_2 thin film. SmF_3-doped SnO_2 (SFTO) thin films were fabricated using a simplified sol-gel dip coating process. The test results show that the transparent conductive oxide SmF_3 with a 2 mol.% doped SnO_2 film exhibits p-type conductivity. Then, in order to confirm the p-type conductivity, the SFTO thin film sample was used for the p-n junction based on the simple p-n heterojunction (p-SFTO/ n-ZnO:Al) was prepared and the I-V characterization was also investigated in this study.

2. EXPERIMENTAL PREPARATION

2.1. Charateristic measurements

We used Microfigure Measuring Instrument Surfcorder – ET300 to measure the film thickness. The structural characterization of the films was analyzed by X-ray diffraction (XRD) measurements with a Bruker-D8SS diffractometer in a grazing incidence mode, using Cu $K\alpha_1$ radiation. The incident angle was fixed at 0.5^o. The XRD measurements were operated at 40 kV, 100 mA with an angle range (2θ) of $20–80^o$ in steps of 0.04^o and the scanning speed was fixed at 2^o min^{-1}. Surface morphology of the films was investigated by the field-emission scanning electron microscope (FESEM, HITACHI/S–4800) operating at 3 kV voltage. A spectrophotometer (Shimadzu UV 1601) was used to measure the optical parameters. The electrical resistivity and Hall effect measurements were carried out using a facility provided by Jiehan Technology Corporation, Taiwan. The electrical resistivity was measured using a four-point probe method. The Hall effect data were measured using a Hall probe on a printed circuit board under a magnetic field 0.53 T, conforming to the van der Pauw configuration. The Seebeck coefficient measurements were performed to verify the conduction type of the films. For the Seebeck coefficient measurements, pairs of micro-heaters and thermocouples were applied to control and measure the temperature difference (ΔT; 300–345K) between two specific points on the sample. At the same moment, through a pair of thin Cu wires, the Seebeck voltages (ΔV) between these two points were detected via the Keithley 2700 data acquisition system. Finally, the Seebeck coefficient ($\Delta V/\Delta T$) was acquired. I–V characteristics was measured using a semiconductor testing system (Keithley 2700).

2.2. Experimental materials

In order to prepare the gel solution, a mixture containing 0.7M tin chloride penta-hydrate ($SnCl_4{\cdot}5H_2O$, Acros Organics, purity 99.0%), 0.7M monoethanolamine (MEA, [C_2H_7NO], Sigma–Aldrich, purity 99%) was dissolved in 2-methoxyethanol ([$C_3H_8O_2$], Sigma–Aldrich, purity 99.5%) as the first solution. Here, tin chloride penta-hydrate, monoethanolamine and 2-methoxyethanol play the roles of tin source, stabilizer, and solvent, respectively. The first solution was stirred for 3 h at 80 °C, and a yellowish and clear solution was obtained.

SmF_3 (Acros Organics, purity 99.9%) were used as the source of Samarium and fluorine dopants, respectively. The quantity of 2 mol.% of SmF_3 were added separately to the beakers containing the first solution. To help complete dissolution of SmF_3 into the first solution, 5 mol/L nitric acid (HNO_3, Sigma–Aldrich, 71%) was also added to the solution. The prepared solution was stirred for 3 h at 80 ^oC. Then, the solution was aged for 7 days at room temperature. Finally, a transparent and yellowish solution was obtained. Un–doped and SmF_3 co-doped SnO_2 thin films were deposited on the glass substrate, Corning EAGLE XG™, by dip-coating method. The substrate was cleaned with a detergent and carefully rinsed with deionized water, then cleaned in boiling water for 15 min. Finally, the substrate was ultrasonicated in a mixture of acetone and ethanol for 20 min and afterward in deionized water for 20 min. The substrate was dipped into the prepared solution for 1 min and then pulled out vertically at a fixed velocity of 3.5 cm/min. The samples were dried at 130 ^oC for 10 min to evaporate the solvent and remove the residual organic materials. They were naturally cooled to room temperature. This procedure was repeated 6 times for thickening the film. The dried films were post-annealed in air at 475 °C for 1 h. Simultaneous, a p-n heterojunction was fabricated by sputter depositing a 100 nm thick layer of the 2 mol.% Al-doped ZnO (ZnO: Al) onto a sol-gel derived 2 mol.% SmF_3-doped SnO_2 thin film with a thickness about 200 nm. Indium was used as the electrode on both p-type and n-type layers.

3. RESULTS AND DISCUSTION

3.1. Structural analysis of the films

The thickness of post-annealed SnO_2 films is revealed in table 1. The thickness of the un-doped SnO_2 film is 228 nm. Considering the same dipping times, the thickness of SmF_3-doped SnO_2 (SFTO) films slightly increases to 238 nm.

Table 1. *Thickness, full–width–at–half–maximum, crystallite size, optical transmittance, and optical band gap of un-doped and 2 mol.% SmF_3 doped SnO_2 thin films prepared by sol–gel dip coating on a glass substrate and post-annealed at 475 ^oC.*

Film	Thickness (nm)	FWHM (degree)	Crystallite size (nm)	Transmittance % @ 550 nm	Optical bandgap (eV)
SnO_2	228	0.575	18	88.8	3.95
SFTO	238	0.483	21	74.3	3.63

Figure 1 depicts the XRD patterns of the SnO_2 film after annealing. The diffraction pattern confirms the presence of a tetragonal rutile structure for the film with major peaks of (110), (101), (200), (211), (220), (301) and (321), and the preferred direction along the plane (110). This indicates that the film has a random orientation consistent with the powder sample (JCPDS #41-1445) [11].

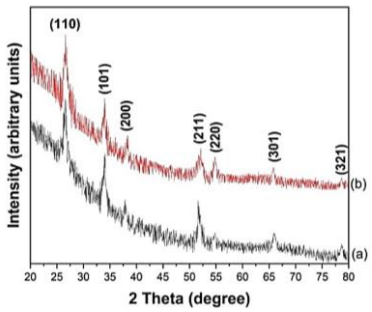

Figure 1. *X-ray diffraction patterns: (a) un-doped SnO_2; (b) 2 mol.% SmF_3-doped SnO_2 [11].*

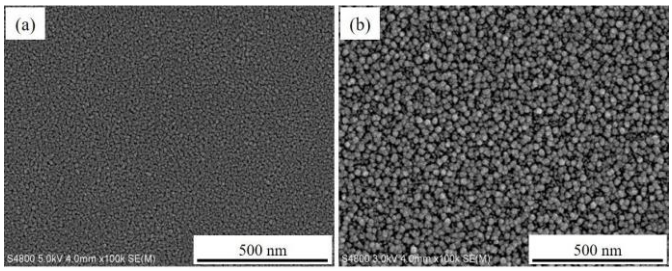

Figure 2. *SEM surface morphology of post-annealed rare-earth fluoride-doped tin oxide films: (a) un-doped SnO_2; (b) 2 mol.% SmF_3-doped SnO_2.*

The full half width maximum (FWHM) inferred from the top (110) of the film is presented in table 1. The FWHM of the SFTO film is slightly reduced compared with that of the undoped SnO_2 film. The crystal size of the undoped SnO_2 film and doped with SmF_3 for the peak (110) was calculated using Scherrer's formula.

$$D = \frac{0,9\lambda}{\beta cos\theta} \quad (1)$$

where D is the crystallite size, λ the wavelength of X-rays used, β full width at half maximum (FWHM) of the diffraction peak and θ is the Bragg diffraction angle. Table 1 collects the calculated crystal sizes. The crystal size of the undoped SnO_2 grain was 18 nm, increasing to 21 nm when doped with 2 mol.% SmF_3.

The surface morphology of the undoped and SmF_3 doped SnO_2 thin films are shown in figure 2. These films are composed of dense particles of nm size. The surface morphology of all films was uniform and there were no detectable cracks. It was observed that the change in the grain structure, grain size and shape of the SmF_3-doped SnO_2 film was compared with that of the undoped SnO_2 film, which is consistent with the XRD results in figure 1. With the results in figure 1. At the same time, looking at the X-ray diffraction pattern in figure 1, we see that the diffraction of planes (211), (321) of the SFTO film has a decrease compared to that of the undoped SnO_2 film, which also proves that Sm^{3+} introduced into the lattice site Sn^{4+} decreases with percentage doping.

3.2. Optical properties of the films

Figure 3 shows the optical transmittance spectrum of the SnO_2 film at 2%.mol SmF_3 doping concentration and the undoped SnO_2 film. All transmittance values were collected at room temperature in air from wavelengths 190 nm to 1100 nm. The concentration of SmF_3 markedly affects the optical transmittance, as shown in figure 3.

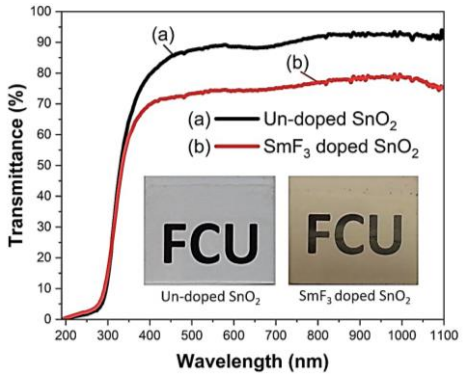

Figure 3. *Transmittance spectra of post-annealed Samarium-trifluoride-doped tin oxide films.*

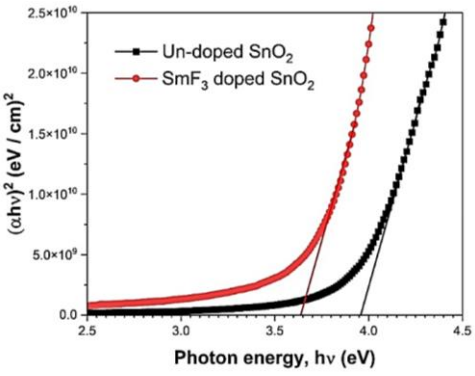

Figure 4. *Optical bandgap (Eg) estimated from the Tauc equation.*

The optical transmittance decreases sharply at wavelengths from 350 nm to 310 nm due to the initiation of elementary absorption. The undoped SnO_2 film exhibits high transmittance (88.8%), as observed at 550 nm. The transmittance of the SFTO film was reduced to 74.3%. The decrease in optical transmittance of SFTO films is attributed to the increased film thickness compared with undoped SnO_2 films, resulting in more light absorption [12]. This can be explained because the higher the defects, the more light is trapped at the defect sites and thus the absorption in the SmF_3:SnO_2 film is improved [13]. The digital photos of un-doped and SmF_3-doped SnO_2 samples was also added inside the Fig. 3. It is easy to see the FCU letters behind the samples. However, the letters are seen less clearly at the SmF_3-doped SnO_2 sample due to its lower optical transmittance. The transmittance in this study is comparable with those reported for other p-type

TCOs; e.g. 88% for $AlSnO_2$ films prepared by spray pyrolysis [14], > 70% for LaCuOS by sputtering radiofrequency [15], > 77% for (Cr_2O_3:Ni) by deposited on the sapphire substrates using pulsed laser deposition (PLD) technique [16].

Figure 4 is a plot of $(\alpha h\gamma)^2$ for undoped SnO_2 and SFTO films as a function of photon energy ($h\nu$). The Tauc's equation is frequently employed to estimate the optical band gap energy of semiconductor thin films [17].

$$(\alpha h\nu) = K(h\nu - E_g)^{1/2} \quad (2)$$

where α is the absorption coefficient, which can be evaluated through the Lambert's law from the transmittance data; K is an energy-independent constant; hν is the photon energy; For example, for undoped SnO_2 and SFTO films the bandgap energy is obtained by extrapolating the straight-line part of the curve from the graph of $(\alpha h\nu)^2$ against photon energy such that the photon energy axis is at $(\alpha h\nu)^2 = 0$. In table 1, the optical band gap is 3.95 eV for undoped SnO_2, which decreases slightly to 3.63 eV when 2 mol.% SmF_3 is added, respectively. Our results are compared with previous studies (3.6–4.0) eV [18].

3.3. Electrical properties of the films

Various electrical properties such as carrier concentration (n), carrier mobility (μ), and resistivity (ρ) was measured by Hall effect measurement in Van der Pauw configuration at room temperature and conductivity type was measured by Seebeck coefficient, measured values are shown in table 2. The undoped SnO_2 thin film nature exhibiting n-type conductivity as determined by the negative sign of the Hall coefficient is explained by the presence of oxygen and tin interstitial voids. The SnO_2:SmF_3 thin film changes conductivity from n-type to p-type when the doping content is 2 mol.% SmF_3 because the increased Sm^{3+} ion is substituted for the activated Sn^{4+} ion as an effective acceptor providing the hole to compensate for the carrier electron caused by intrinsic defects in SnO_2, the acceptor energy level is generated near the valence band, thus increasing the hole concentration and is the majority carrier in thin films SnO_2:SmF_3. For example, several studies have been published; the critical impurity doping level at which the conductivity type changes from n-type to p-type for sol-gel derived SnO_2:Al thin films has been reported to be 12.05 mol.% [19]. As shown in table 2, the SnO_2 film is phaseless. Dopants with a Seebeck coefficient of –171 μV/K indicate an n-type conductive film. When 2 mol.% SmF_3 is doped into the SnO_2 film, there are positive values of the Seebeck coefficient, which is +120 μV/K. This demonstrates that films with p-type conductivity. From table 2, it can also be seen that the Seebeck coefficient of the SFTO film decreases, which are inversely proportional to the hole concentration. The trend follows the reciprocal relationship between the carrier concentration (n) and the Seebeck coefficient (S), given by Equation [20].

$$S = \frac{8\pi^2 k_B^2}{3eh^2} m^* T \left(\frac{\pi}{3n}\right)^{2/3} \quad (3)$$

where m* is the effective mass of the carrier.

Table 2. *Electrical properties of un-doped and 2 mol.% SmF_3 doped SnO_2 thin films post-annealed at 475 ^oC.*

Film	Resistivity, Ω cm	Carrier Conc. cm^{-3}	Hall mobility, $cm^2\ V^{-1}\ s^{-1}$	Seebeck Coeff. $\mu V\ K^{-1}$	Type of elec. conductivity
SnO_2	2.37×10^{-2}	-9.34×10^{18}	28.20	–171	n
SFTO	7.83×10^{-3}	$+1.05 \times 10^{20}$	7.57	+120	p

In figure 5, the SFTO film showed reduced resistivity and Hall mobility while the hole concentration increased compared with the undoped SnO_2 film. The decrease and change in resistivity of the SFTO film in this study is due to the increase and change in carrier

concentration [7]. The undoped SnO_2 film has a carrier concentration of -9.34×10^{18} cm^{-3}. The concentration of this carrier increased many times when 2 mol.% SmF_3 was added to the SnO_2 film and reached a value of 1.05×10^{20} cm^{-3}. One possible mechanism of increased carrier concentration with SmF_3-doped SnO_2 films could arise from the substitution of the Sm^{3+} site to the Sn^{4+} site and the F– site to the O_2– site, thereby generating acceptor levels in the network. The mechanism may be due to SmF_3 doping and is explained by the Kröger–Vink notation [21].

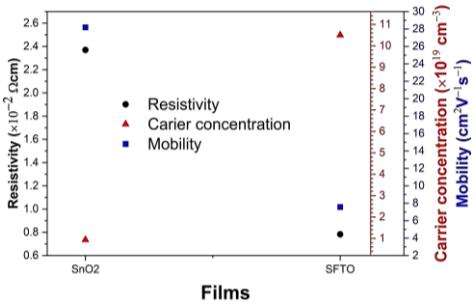

Figure 5. *Variation in electrical resistivity, carrier concentration, and Hall mobility of Samarium trifluoride-doped tin oxide films.*

3.4. Properties of p-type SFTO/n-type AZTO heterojunction

To confirm the p-type conductivity of the SmF_3-doped SnO_2 thin film, a p-type (SnO_2:SmF_3)/n-type ZnO (ZnO:Al)-doped SnO_2 heterojunction was fabricated on a Corning EASE glass substrate. XG™. The bandgap energy diagram of the p-n heterodiode consisting of the p-type semiconductor thin films SnO_2:SmF_3 and n-type ZnO:Al is shown in figure 6. We know that the values of the basic bandgap for SnO_2 and ZnO is about 3.6 eV and 3.4 eV at room temperature, and their electron affinity is about 4.5 eV and 4.3 eV, respectively [22]. Since SnO_2:SmF_3 is a p-type semiconductor due to its high hole concentration, the Fermi level (E_f) shifts towards the valence band (E_v); ZnO:Al is an n-type semiconductor, so the Fermi level (E_f) shifts towards the conduction band (E_c). Figure 7 - Schematic depiction of the structure of the p-n heterojunction is illustrated on the left, the right figure shows the I-V curve measured from a pair of contacts indium spot on p-type and n-type materials. The observed results in figure 7. show that the I-V curve of the superimposed structure of SnO_2:SmF_3/ZnO:Al is non-linear, similar the I–V characteristics of the SnO_2 homojunction, which is consistent with the formation of a p-n junction at the interface fabricated by deposition pulsed laser [23]. This feature clearly shows the formation of a p-n junction at the interface and shows a forward turn-on voltage of 1.55 V.

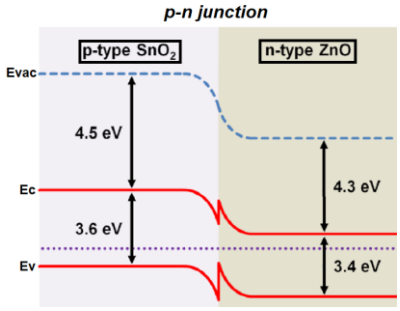

Figure 6. *Band gap energy diagram of a p-n heterojunction diode.*

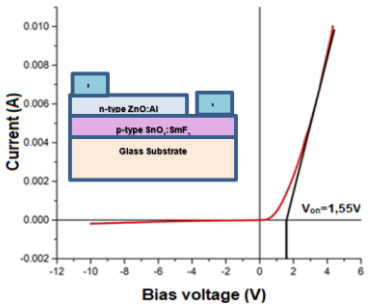

Figure 7. *I–V characteristics of p-type SFTO/n-ZnO:Al heterojunction. The insets show a schematic diagram of p–n heterojunction (upper left) and the I-V characteristics of In contact on the p-type and n-type (upper right).*

4. CONCLUSIONS

Conduction type, structure, electrical and optical properties of the SFTO films were investigated. The conduction type of the films is converted from n-type for un-doped- to p-type for SmF_3 doped-SnO_2 film. Such conversion is confirmed by both Hall effect and Sebeck coefficients measurements. The p-type SFTO film shows high transmittance of 74.3% with band gap 3.63 eV. Resistivity, carrier concentration, and Hall mobility of SFTO films reached values of 7.83×10^{-3} Ωcm, $+1.05 \times 10^{20}$ cm^{-3}, and 7.57 cm^2 V^{-1} s^{-1}, respectively, which revealed an improvement in electrical properties of doped films. Furthermore, p-type conductivity of the 2 mol.% SmF_3-doped SnO_2 thin film was also confirmed by the non-linear I-V characteristics of the p-type SnO_2:SmF_3/n-type ZnO:Al heterojunction. The turn-on voltage of the p-n heterojunction diode were found to be 1.55 V. These results show that p-type SFTO films have bright applications in optoelectronic devices.

Acknowledgements: *This research is funded by Hung Yen University of Technology and Education under grand number UTEHY.L.2021.01.*

REFERENCES

[1]. S. C. Dixon, D. O. Scanlon, C. J. Carmalt, and I. P. Parkin, *"n-Type doped transparent conducting binary oxides: an overview,"* Journal of Materials Chemistry C, vol. 4, no. 29, pp. 6946-6961, (2016).

[2]. C. P. Liu *et al.*, *"Room-Temperature-Synthesized High-Mobility Transparent Amorphous CdO-Ga(2)O(3) Alloys with Widely Tunable Electronic Bands,"* ACS Appl Mater Interfaces, vol. 10, no. 8, pp. 7239-7247, (2018).

[3]. M. Ahmadi, M. Asemi, and M. Ghanaatshoar, *"Mg and N co-doped $CuCrO_2$: A record breaking p-type TCO,"* Applied Physics Letters, vol. 113, no. 24, (2018).

[4]. K. Jenifer, S. Arulkumar, S. Parthiban, and J. Y. Kwon, *"A Review on the Recent Advancements in Tin Oxide-Based Thin-Film Transistors for Large-Area Electronics,"* Journal of Electronic Materials, vol. 49, no. 12, pp. 7098-7111, (2020).

[5]. K. Hui, K. S. Hui, L. Li, Y. Cho, and J. Singh, *"Low resistivity p-type $Zn_{1-x}Al_xO$:Cu_2O composite transparent conducting oxide thin film fabricated by sol–gel method,"* Materials Research Bulletin, vol. 48, no. 1, pp. 96–100, (2013).

[6]. K. Ravichandran, K. Thirumurugan, N. Jabena Begum, and S. Snega, *"Investigation of p-type SnO_2:Zn films deposited using a simplified spray pyrolysis technique,"* Superlattices and Microstructures, vol. 60, pp. 327-335, (2013).

[7]. P. Sakthivel, S. Asaithambi, M. Karuppaiah, S. Sheikfareed, R. Yuvakkumar, and G. Ravi, *"Different rare earth (Sm, La, Nd) doped magnetron sputtered CdO thin films for optoelectronic applications,"* Journal of Materials Science: Materials in Electronics, vol. 30, no. 10, pp. 9999-10012, (2019).

[8]. N. B. A. Bouaine, G. Schmerber, C. Ulhaq-Bouillet, S. Colis, A. Dinia, , *"Structural, Optical, and Magnetic Properties of Co-doped SnO2 Powders Synthesized by the Coprecipitation Technique"*, pp. 2924–2928, (2007).

[9]. C. Li, W. Wei, T. Xia, H. Wang, Y. Zhu, and Y. Song, *"La-doped SnO2 synthesis and its electrochemical property,"* Journal of Rare Earths, vol. 28, pp. 161-163, (2010).

[10]. M. Arif, S. Monga, A. Sanger, P. M. Vilarinho, and A. Singh, *"Investigation of structural, optical and vibrational properties of highly oriented ZnO thin film,"* Vacuum, vol. 155, pp. 662-666, (2018).

[11]. JCPDS Card No. 41–1445 for Tetragonal SnO_2, (2007).

[12]. I. Y. Y. Bu, *"Sol–gel deposition of fluorine-doped tin oxide glasses for dye sensitized solar cells,"* Ceramics International, vol. 40, no. 1, pp. 417-422, (2014).

[13]. N. B. Ibrahim, M. H. Abdi, M. H. Abdullah, and H. Baqiah, *"Structural and optical characterisation of undoped and chromium doped tin oxide prepared by sol–gel method,"* Applied Surface Science, vol. 271, pp. 260-264, (2013).

[14]. C. Benouis *et al.*, *"The low resistive and transparent Al-doped SnO_2 films: p-type conductivity, nanostructures and photoluminescence,"* Journal of Alloys and Compounds, vol. 603, pp. 213–223, (2014).

[15]. K. Ueda, S. Inoue, S. Hirose, H. Kawazoe, and H. Hosono, *"Transparent p-type semiconductor: LaCuOS layered oxysulfide,"* Applied Physics Letters, vol. 77, no. 17, pp. 2701–2703, (2000).
[16]. J. Singh, R. Kumar, V. Verma, and R. Kumar, *"Structural and optoelectronic properties of epitaxial Ni-substituted Cr_2O_3 thin films for p-type TCO applications,"* Materials Science in Semiconductor Processing, vol. 123, (2021).
[17]. Q.-P. Tran, J.-S. Fang, and T.-S. Chin, *"Properties of fluorine-doped SnO_2 thin films by a green sol–gel method,"* Materials Science in Semiconductor Processing, vol. 40, pp. 664–669, (2015).
[18]. F. Arefi-Khonsari, N. Bauduin, F. Donsanti, and J. Amouroux, *"Deposition of transparent conductive tin oxide thin films doped with fluorine by PACVD,"* Thin Solid Films, vol. 427, no. 1-2, pp. 208–214, (2003).
[19]. S. F. Ahmed, S. Khan, P. K. Ghosh, M. K. Mitra, and K. K. Chattopadhyay, *"Effect of Al doping on the conductivity type inversion and electro-optical properties of SnO_2 thin films synthesized by sol-gel technique,"* Journal of Sol-Gel Science and Technology, vol. 39, no. 3, pp. 241-247, (2006).
[20]. E. S. T. G. J. Snyder, *"Complex thermoelectric materials" in materials for sustainable energy: a collection of peer-reviewed research and review articles from Nature Publishing Group,"* World Scientific, pp. 101–110., (2011).
[21]. F. A. Kröger, *"The Chemistry of Imperfect Crystals: Imperfection Chemistry of Crystalline Solids"*. North-Holland Publishing Company (etc.), (1974).
[22]. F. M. Hossain *et al.*, *"Modeling and simulation of polycrystalline ZnO thin-film transistors,"* Journal of Applied Physics, vol. 94, no. 12, (2003).
[23]. S. Yu, W. Zhang, L. Li, D. Xu, H. Dong, Y. Jin, *"Fabrication of p-type SnO_2 films via pulsed laser deposition method by using Sb as dopant,"* Applied Surface Science, vol. 286, pp. 417-420, (2013).

TÓM TẮT

Tính chất cấu trúc, điện và quang của màng mỏng oxit dẫn điện trong suốt SnO_2 pha tạp SmF_3 cho các ứng dụng thiết bị quang điện tử

Trong nghiên cứu này, các màng mỏng bán dẫn chứa oxit thiếc (SnO_2) trong suốt loại p được lắng đọng trên đế thủy tinh bằng phương pháp phủ nhúng sol-gel sử dụng samarium-triflorua (SmF_3) làm chất tạp nhận. Các màng này được điều chế bằng cách đồng pha tạp 2 mol.% SmF_3 vào SnO_2 (SFTO), tiếp theo là nhiệt độ ủ ở 475 $^{\circ}C$. Kết quả phân tích XRD cho thấy màng thể hiện pha rutile tứ phương SnO_2. Độ dẫn loại p của màng SFTO được xác định bằng phép đo hiệu ứng Hall và hệ số Seebeck. Điện trở suất và độ linh động của màng SnO_2 pha tạp SmF_3 lần lượt là 7.83×10^{-3} Ωcm và $7.57\ cm^2\ V^{-1}\ s^{-1}$, giảm so với màng SnO_2 không pha tạp. Nồng độ chất mang tăng lớn từ -9.34×10^{18} cm^{-3} đối với màng không pha tạp đến $+1.05 \times 10^{20}\ cm^{-3}$ đối với màng SnO_2 pha tạp SmF_3. Màng SFTO loại p cho thấy độ truyền qua cao 74.3% ở bước sóng 550 nm, với năng lượng vùng cấm là 3.63 eV. Ngoài ra, một dị thể p-SnO_2:SmF_3/n-ZnO:Al (mức pha tạp Al là 2 mol.%) trong suốt được chế tạo trên đế thủy tinh không chứa kiềm. Phép đo đường cong I-V đối với đi-ốt dị vòng p-n cho thấy đặc tính chỉnh lưu điển hình với điện áp mở thuận là 1.55 V. Với các đặc tính thu được, màng SFTO loại p hứa hẹn rất nhiều cho các ứng dụng thiết bị quang điện tử.

Từ khoá: Màng SnO_2 pha tạp SmF_3; Oxit dẫn điện trong suốt (TCO); Nhúng phủ Sol–gel; Điện trở suất; TCO loại p.